Supporting information

High efficiency quantum-dot light-emitting diodes enabled by boosting hole injection

Chunyan Cheng[1], Aqiang Liu[1], Guohang Ba[1], Ivan S. Mukhin[2], Fei Huang[1], Regina M. Islamova[3], Wallace C. H. Choy[4], and Jianjun Tian[1].*

[1]Institute for Advanced Materials and Technology, University of Science and Technology Beijing, Beijing 100083, China

[2] Laboratory of Renewable Energy Sources, St. Petersburg Academic University, St. Petersburg, 194021 Russian Federation

[3]Institute of Chemistry, St. Petersburg State University, St. Petersburg, 199034 Russian Federation

[4]Department of Electrical and Electronic Engineering, The University of Hong Kong, Pokfulam Road, Hong Kong, 999077, China

*E-mail: tianjianjun@mater.ustb.edu.cn

Experimental section

Chemicals and materials: Tetramethylammonium hydroxide pentahydrate (TMAH, ≥ 97 %), Poly(9-vinylcarbazole) (PVK), Ethylacetate (≥ 99.5 %) and Dimethyl sulfoxide (DMSO, 99 %) were purchased from sigma-aldrich. Chlorobenzene (≥ 99.5 %) was purchased from Aladdin. Ethanol (≥ 99.8 %) and Zinc acetate·$2H_2O$ (Zn(Ac)·$2H_2O$, 99.99 %) were purchased from Macklin. Magnesium acetate tetrahydrate ($Mg(Ac)_2·4H_2O$, 98 %-102 %) was purchased from Alfa Aesar. The red CdSe@ZnS QDs was purchased from Mesolight Inc. Patterned ITO-coated glasses (20 Ω sq^{-1}) were purchased from Xin Yan Technology Ltd. Poly[(3,4-ethylenedioxythiophene)-poly(styrenesulfonate) dry redispersiblepellets] (PEDOT: PSS) and Poly[(9,9-dioctylfluorenyl-2,7-dily)-alt-(4,4'-(N-(4-butylphenyl)] (TFB) were purchased from Xi'an Polymer Light Technology Corp. All of the materials were used without any further purification.

Synthesis of ZnMgO nanoparticles: Firstly, 0.0320 g $Mg(Ac)_2·4H_2O$ and 0.2960 g Zn(Ac)·$2H_2O$ were dissolved in 15 mL DMSO under stirring. After the solution is dissolved, it is heated to 50 °C. Secondly, 0.3430 g TMAH was dissolved in 5mL ethanol under stirring. Thirdly, the solution of TMAH was added to the above solution at a rate of 0.75 mL/min. The mixture was reacted for 1h at 50 °C. The reacted solution was washed with ethyl acetate at 4000 rpm for 3 min.

Fabrication of QLEDs devices: The QLEDs were fabricated in the nitrogen-filled glovebox, except the PEDOT: PSS layer was spin-coated in the air atmosphere. The ITO substrates were rubbed with cleaning powder, ultrasonic by deionized water, acetone, and ethanol for 20 min, respectively. Then, the ITO substrates were dried by nitrogen and transferred into the UV ozone cleaner, and treated for 30 min. PEDOT: PSS (Baytron PVP Al 4083, filtered through a 0.45 mm N66 filter) was spin-coated at 3500 rpm for 45 s and annealed at 140 °C for 10 min. HTLs (TFB, PVK, or TFB blended with PVK (P-HTL)) in chlorobenzene with the concentration of 12 mg / mL was spin-coated at 2500 rpm for 45 s and annealed at 130 °C for 25 min. CdSe@ZnS

QDs in octane with a concentration of 20 mg / mL were spin-coated at 2000 rpm for 45 s and annealed at 90 °C for 10 min. ZnMgO QDs for the ETL layer was spin-coated at 2500 rpm for 45 s and annealed at 100 °C for 10 min. The Ag electrode was deposited in the thermal evaporation system under a vacuum of 4.0×10^{-4} Pa, at a rate of 1 Å / s for the first 50 Å, and 3 Å / s for the last 650 Å.

Fabrication of the hole-only devices (HOD): The HOD with the structure of ITO / PEDOT: PSS / HTL / CdSe@ZnS QDs / MoO_3 / Ag was prepared, with the thickness of each layer equal to that of the complete device. The MoO_3 layer with a thickness of 6 nm was deposited.

Characterizations

Atomic force microscope (AFM) was characterized on an MFP-3D Infinity AFM (Asylum Research, Oxford Instruments). The Grazing incidence X-Ray diffraction (GIXRD) data were carried out with a Xeuss 2.0 SAXS/WAXS laboratory beamline using a Cu X-ray source and the Pilatus3R 300K detector. The incidence angle is 0.15°. Powder X-ray diffraciton (PXRD) was performed on MXP21VAHF X-ray diffractometer using Cu Kα RADIATION (λ = 1.5418 Å). The ultraviolet photoelectron spectroscopy (UPS) measurement was performed on the PHI5000 VersaProbe III (Scanning ESCA Microprobe) SCA (Spherical Analyzer). Fourier transform infrared (FTIR) spectroscopy was performed on a Varian 3100 FTIR spectrometer. Cross-sectional transmission electron microscopy (STEM) was performed on a JEOL JEM-2010 microscope operated at 200 kV and a Tecnai G2 F30 S-TWIN and Titan TM G2 60-300 TEM instrument operated at 300 kV. Scanning electron microscopy (SEM) was taken by the Helios Nanolab 600i. The performance of the QLEDs were obtained from Keithley 2400 source together with the Photo-Research spectroradiometer (PR655), including the current density (*J*), luminance (*L*), voltage (*V*), and the electroluminescence (*EL*). The contact angles were measured by a measurement system (JY-82B Kruss DSA). The time-resolved photoluminescence (TRPL) spectra were measured by a fluorescence spectrometer (FLS980, Edinburgh).

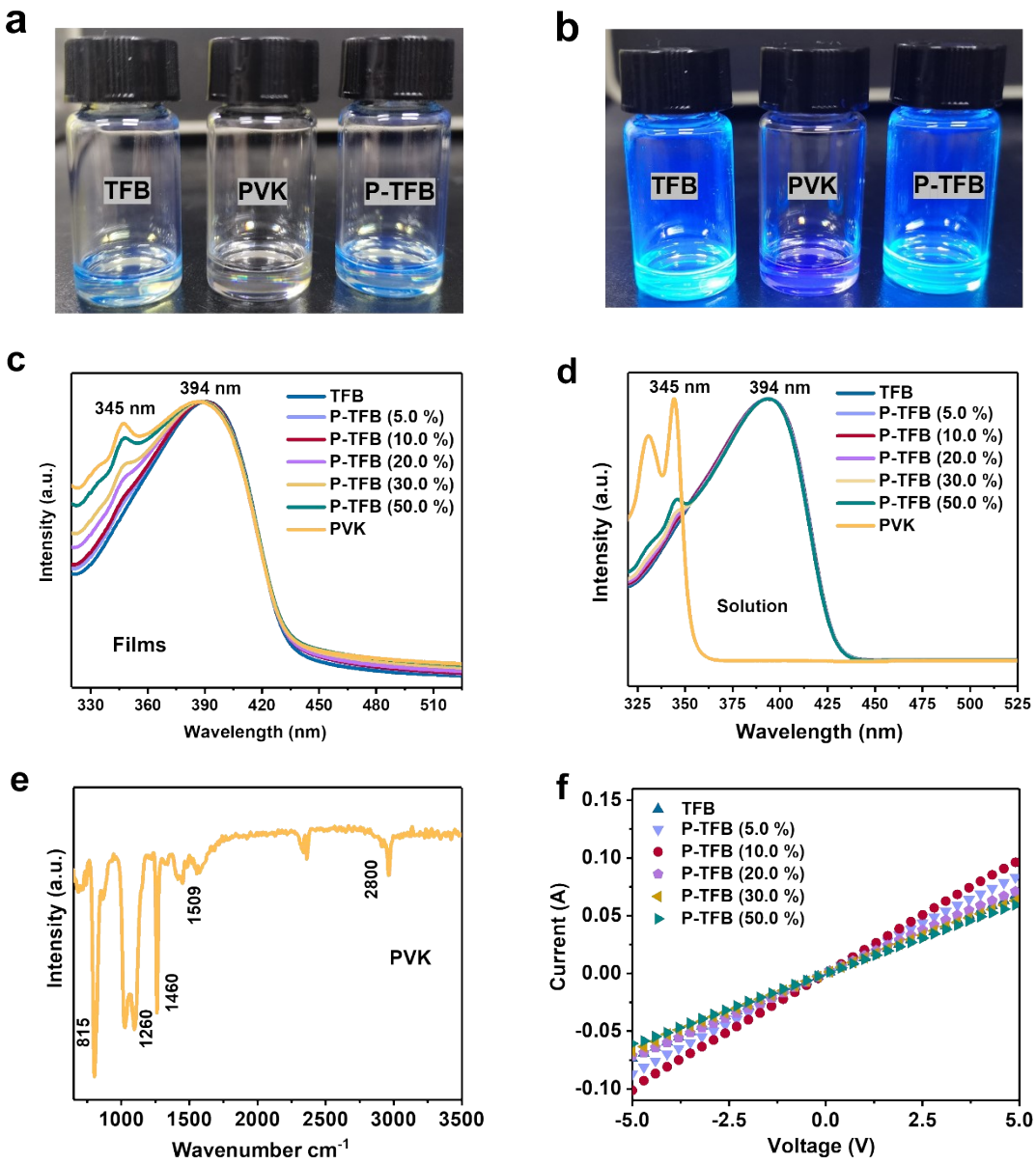

Figure S1 Images of the HTL solutions under **(a)** sunlight and **(b)** UV irradiation. The absorption spectra of the HTL **(c)** films and the **(d)** solutions. **(e)** Fourier transform infrared (FTIR) spectra of the PVK film. **(f)** I-V characteristics of ITO/HTLs/Ag based on HTLs with different mass ratio for PVK.

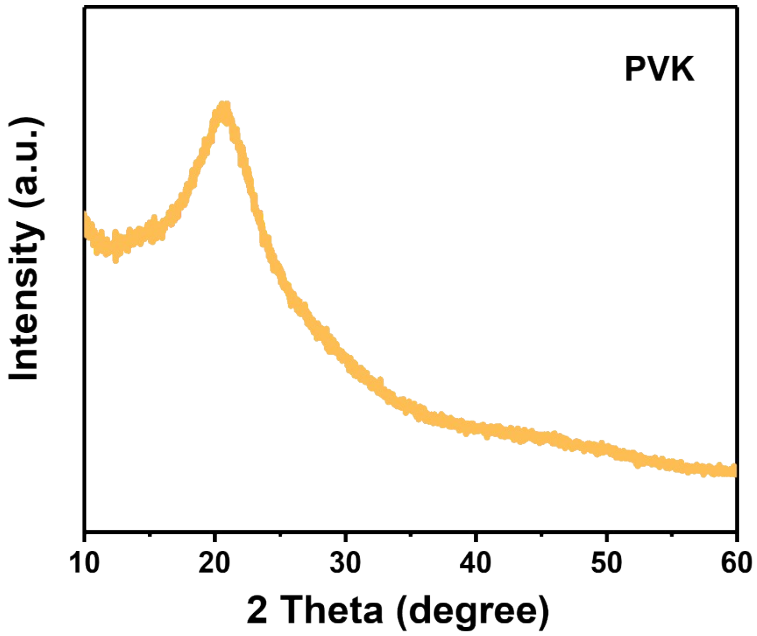

Figure S2 Powder X-ray diffraction (PXRD) of the PVK.

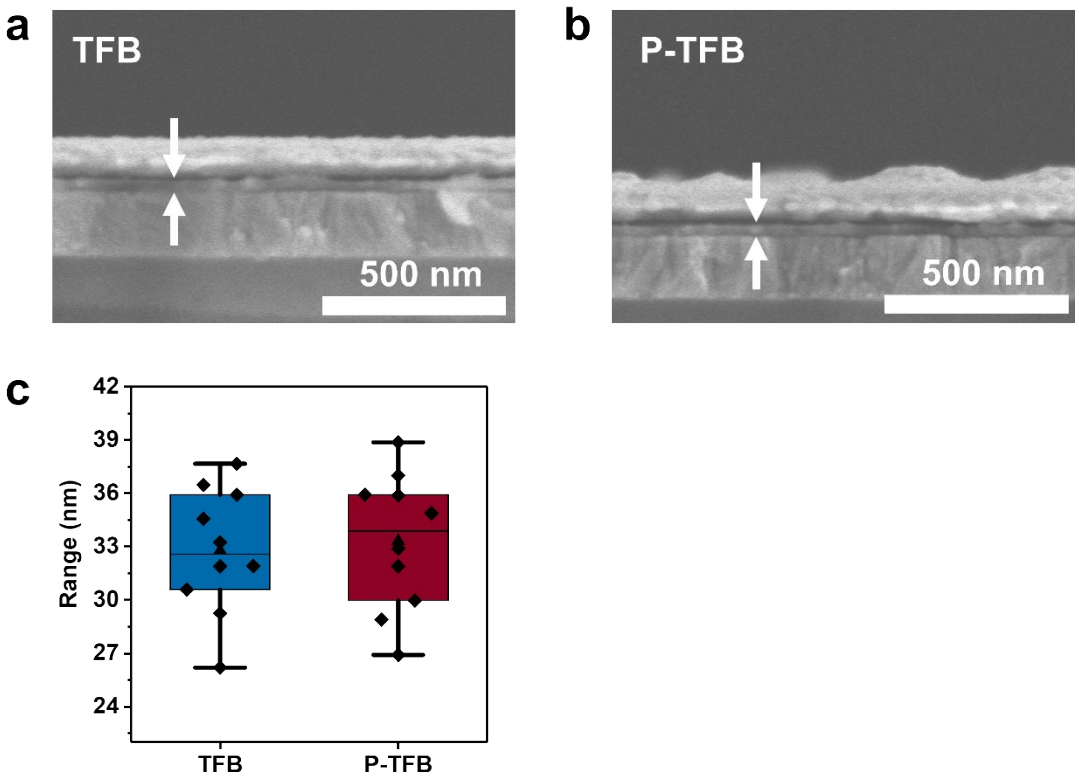

Figure S3 Cross-sectional image of the **(a)** TFB and **(b)** P-TFB layers with structure of ITO/HTL/Ag. **(c)** Thickness statistics of the TFB and P-TFB layers.

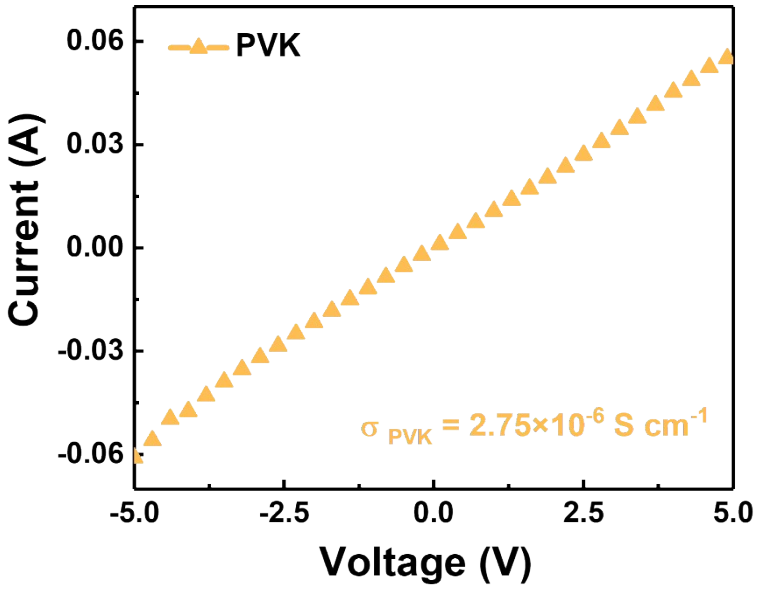

Figure S4 I-V characteristics of ITO/PVK/Ag

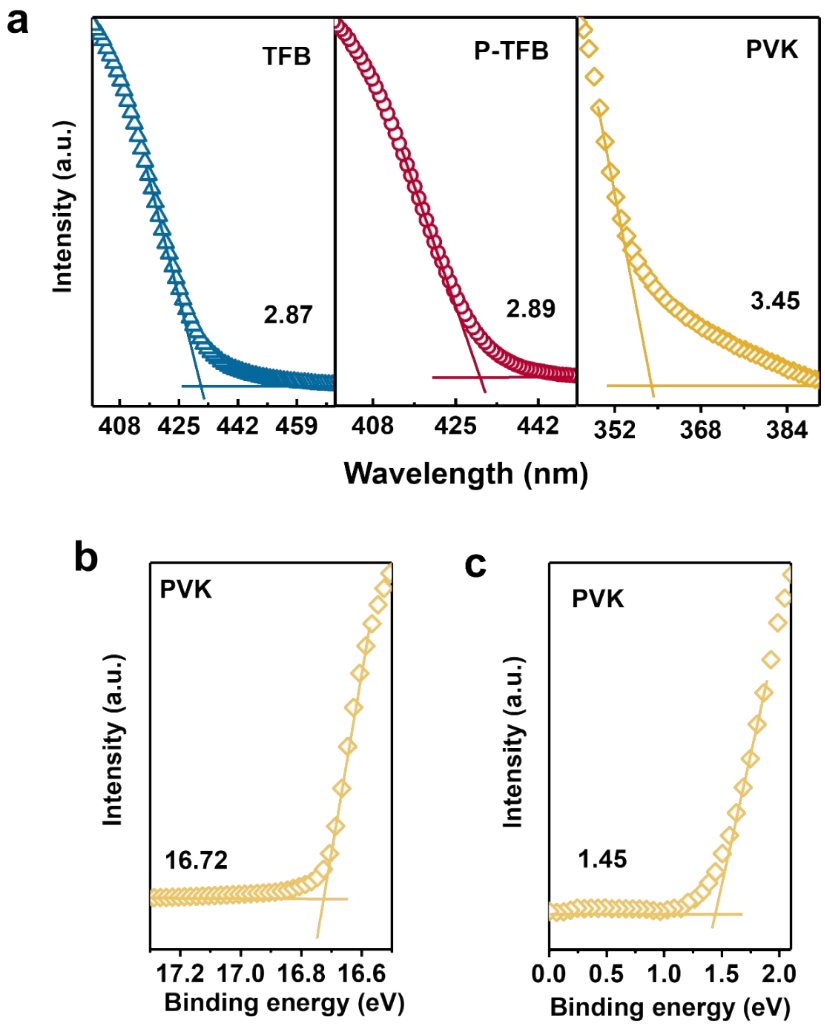

Figure S5 (a) The absorption spectra of the TFB, P-TFB, and PVK films. The **(b)** secondary-electron cutoff (E_{cutoff}) and **(c)** valence-band edge regions (E_{onset}) of the PVK film.

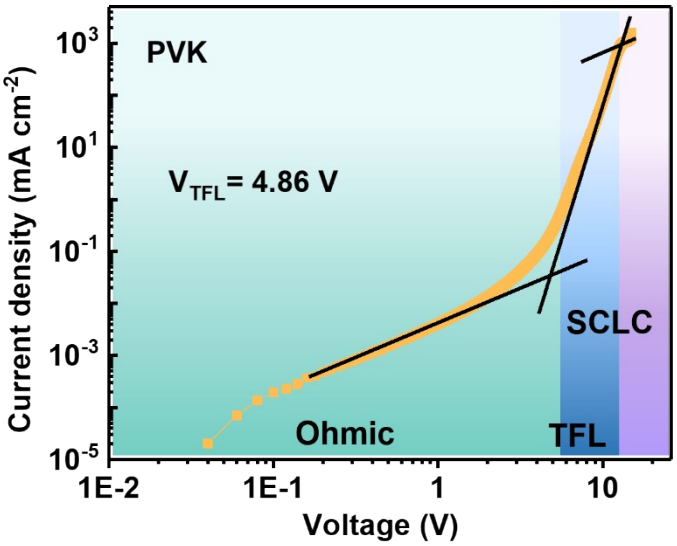

Figure S6 The current density versus voltage curve of the HOD based on the PVK.

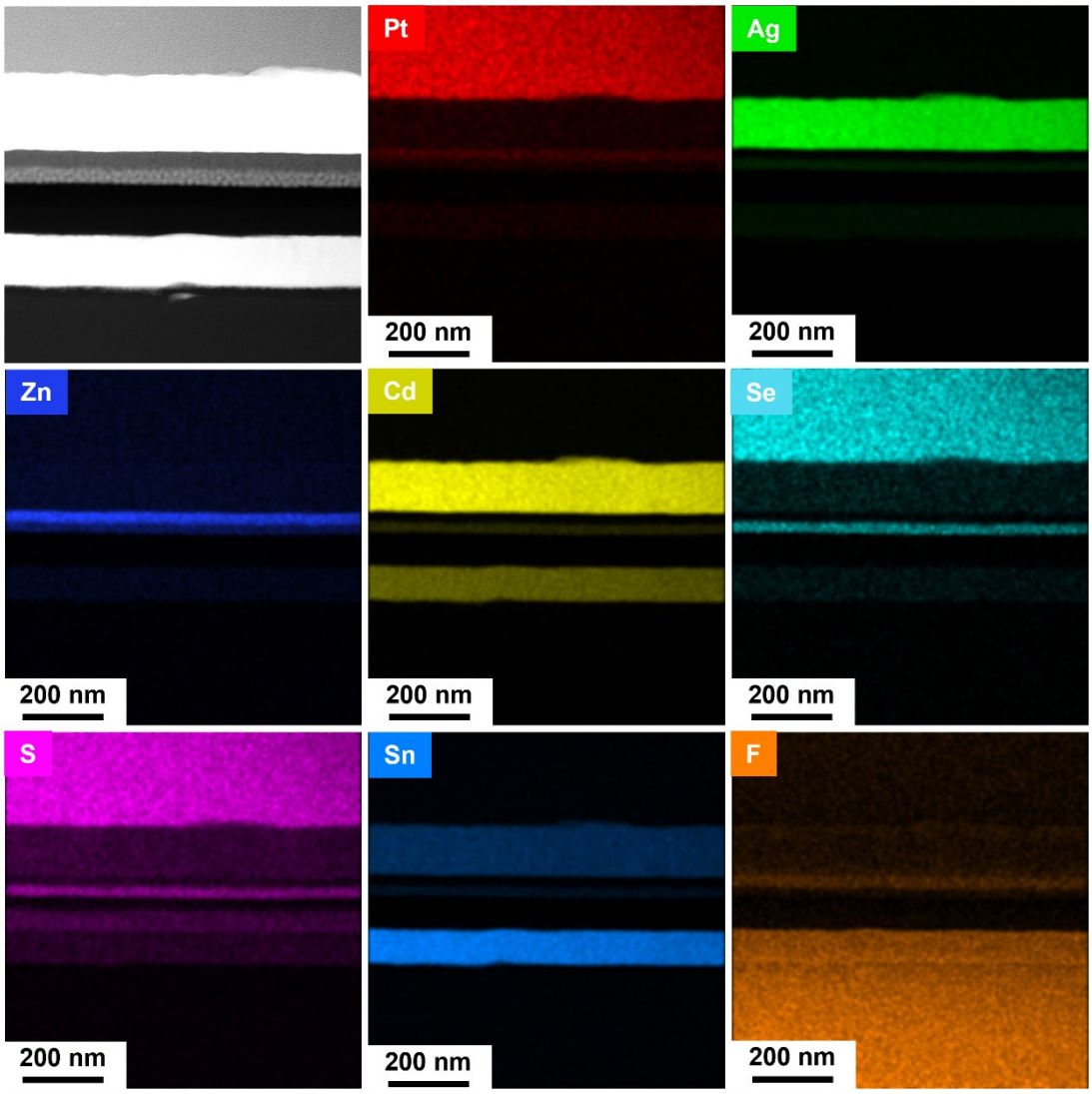

Figure S7 HAADF-STEM images and the corresponding EDS element mapping of multiple layers for the device.

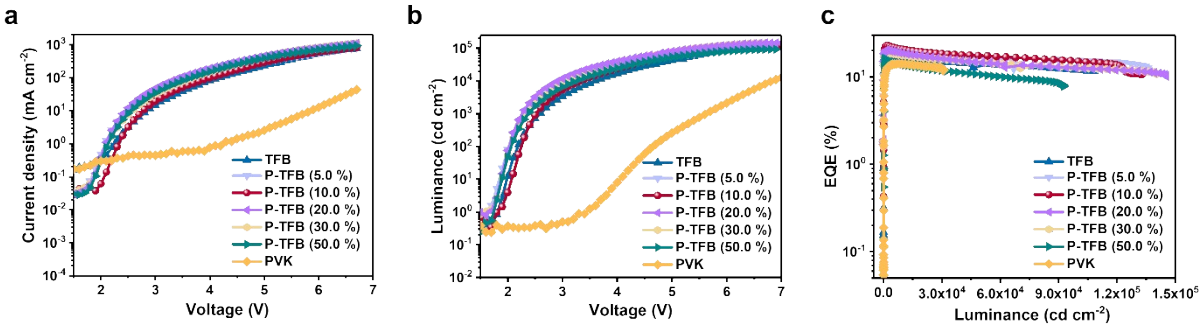

Figure S8 Device performance for QLEDs with different HTL. (a) Current density as a function of voltage for QLEDs. **(b)** Luminance as a function of voltage for QLEDs. **(c)** EQE as a function of luminance for QLEDs.

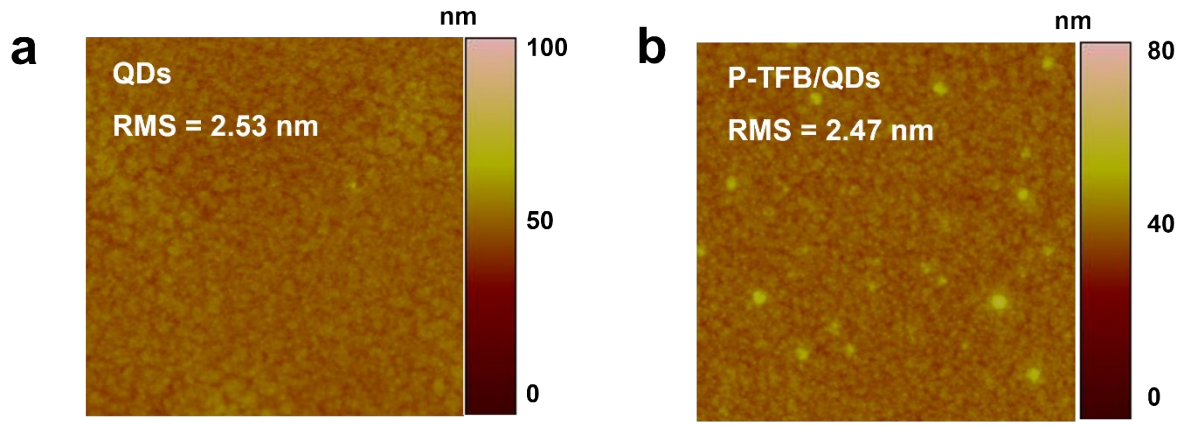

Figure S9 AFM images of the **(a)** QDs film and the **(b)** P-TFB/QDs film.

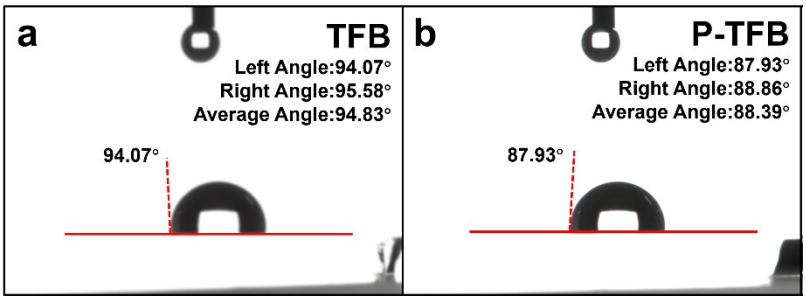

Figure S10 Contact angles of **(a)** the TFB, and **(b)** the P-TFB.

Table S1 Energy characteristics of the TFB, PVK, and P-TFB HTL films.

Film	E_{cutoff} (eV)	WF (eV)	E_{onset} (eV)	HOMO (eV)	E_g (eV)	LUMO (eV)
TFB	17.00	4.20	1.09	5.29	2.87	2.42
PVK	16.72	4.48	1.45	5.93	3.45	2.48
P-TFB	16.87	4.33	1.03	5.36	2.89	2.47

Table S2 Device performance of the HODs with different HTLs.

HTL type	Current density ($mA\ cm^{-2}$)	Voltage (V)	V_{TFL} (V)	N_t (cm^{-3})	μ ($cm^2\ V^{-1}\ S^{-1}$)
TFB	1316.1	9.7	4.72	1.78×10^{21}	1.08×10^{-3}
P-TFB	1654.1	7.8	4.59	1.73×10^{21}	2.09×10^{-3}
PVK	897.7	9.7	4.86	1.83×10^{21}	7.24×10^{-4}

Table S3 Device performance for the QLEDs with different HTL.

HTL	V_T (V)	CE_{max} (cd A^{-1})	$L_{(max)}$ (cd m^{-2})	EQE_{max} (%)
TFB	1.9	23.2	108300	17.6
5.0% PVK	1.8	25.6	136100	19.2
10.0% PVK	1.8	29.3	133100	22.7
20.0% PVK	1.8	25.2	140300	19.3
30.0% PVK	1.8	26.8	145400	20.1
50.0% PVK	1.8	20.7	92710	16.2
PVK	3.5	18.6	30960	14.1